70(10A): 247-253; 2022. DOI: 10.18311/jmmf/2022/31244

Print ISSN : 0022-2755

Journal of Mines, Metals and Fuels

Contents available at: www.informaticsjournals.com/index.php/jmmf

# Fractal Contact Mechanic Behaviour of Base Structural Steels in Abrasion

**Chethan S[1], Srinivasa K[1], Hemanth B R[1], and Hemaraju[2*]**

[1]*Department of Mechanical Engineering, ATME College of Engineering, Mysuru - 570028, Karnataka, India*

[2]*Department of Mechanical Engineering, BGSIT, Adichunchangiri University, BG Nagara - 571418, Karnataka, India; [*]Email: hemarajucrp@gmail.com*

## Abstract

Inelastic behaviour and fracture in the metals act as a major failure leading to permanent breakage of the machine elements. Such a type of failures may cause from variety of loading and forces and tribological behaviour is also one of the phenomena. Tribological failures may cause when two rubbing surfaces are abraded depending on the loading. In the present study abrasion studies were done on the three base structural steels namely mild steel, cast iron, high carbon high chromium steel and heat resistant steel. Materials are subjected varied normal loading, time and different velocities of abrader. Volume loss was found out and inelastic and damage behaviour were studied in scanning electron microscope. It was found that volume loss was depending on hardness and volume loss increases with increasing in normal load and abrader. Various wear modes were found along with little fracture in the subsurface.

**Keywords:** *Tribological behaviour, Abrasion, structural steel, scanning electron microscope etc.*

## 1.0 Introduction

Wear is the surface failure of the material defined in terms of progressive loss or gradual loss during their contact in application. Phenomenonically wear is the process of removal of material removal due to deformation, thermal heating and melting at contact surfaces. It is very difficult to understanding the mechanisms of wear which describes phenomena of wear because of complexity of process during friction. The amount of rate was defined in terms of volume loss/unit distance. Wear coefficients were correlated with hardness of the material amount of wear rate [1-7].

The wear mechanisms gave clear information such as volume loss due to wear, surface roughness and particle shape influencing on wear. There are three types dependencies of wear with respect to time was found. In first type micro structural changes in the material surface which cause deformation. In the second type transformation of wear rate was dependent on the type of wear debris and third one is the stresses and the shearing action performed with opposite rubbing face [8]. Second type was found in metals and third type dependency was found in ceramics [9].

Wear and deformations of metals in machinery, since they affect reliability and performance of the equipment are an important phenomenon. Researchers have attempted conducting laboratory scale experiments for simulating field conditions [10]. Bingley and Schnee attempt to study the mechanisms of abrasive wear of ductile materials under wet and dry three body wear and identified the sliding and cutting mode of wear in target materials, so that the reason is for tensile properties in steel. Yefei Li and Yimin Gao [11] tried to find the influence of composites on metals during the surface contact. They found that the modes of wear are not only depending on type of abrasive, but also on the specific time of surface contact. ErdingWen RenboSong et al [12] tried to study the three body impact abrasive behaviour of

*Corresponding Author

low alloy steel reinforced with niobium and found that reinforced steel shows better wear resistance and reinforcement acts as lubrication on surface during abrasive contact with the steel.

## 2.0 Experimental Set Up

Experiments were conducted using Brinell hardness testing machine and dry sand abrader. The experimental procedures followed as per ASTM standards for both the tests. The schematic diagram dry sand rubber wheel abrasion test rig is shown in the Figure 1.

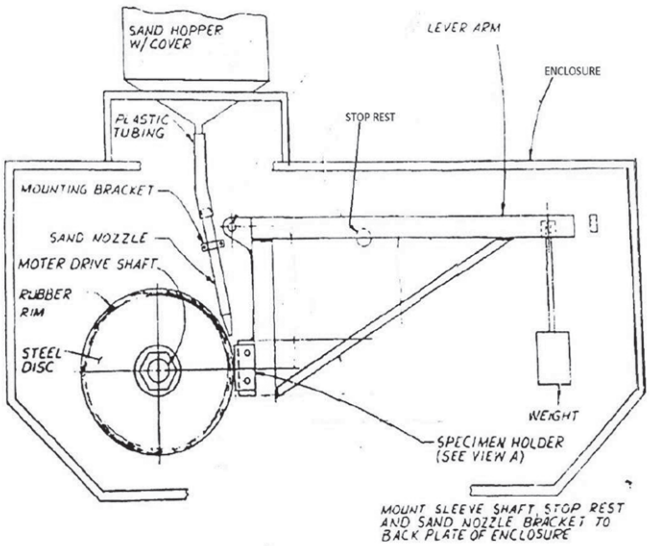


**Figure 1:** Dry sand wheel abrader

Tests carried out by following parameters such as time for the test is taken as 8 minutes. Flow velocity of the abrader was maintaining with 100 grams per minute. The wheel rotation was for all the normal load was maintained with 200 rpm. Two normal loads followed with 53.2 N and 102.4 N was calculated as per the leverage load given in the specimen holder. Specimen was weighed in the weighing machine to find initial volume and fixed to the specimen holder. The hopper is filled with the abrader and allowed to the flow at defined flow rate by rotating the wheel in the specified rpm. After the test specimen was removed from specimen holder and weighed in the weighing machine to found the volume loss. The wear scar happened on the target materials was studied in the scanning electron microscope to identify wear deformation. The target samples were also sectioned for subsurface study. Sectioned surface is shown in Fig.2.

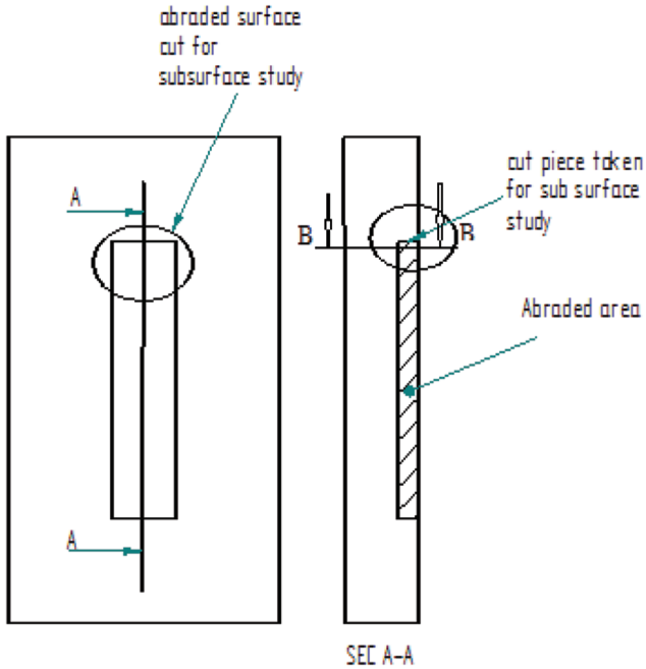


**Figure 2:** Schematic view of specimen prepared for subsurface study

## 3.0 Results and Discussion

### 3.1 Hardness Test

Keeping the displacement and hardness of the target material which characterize the wear modes, experiments were conducted to understand the dependency of wear on hardness and microstructure of the material varies. Target materials selected are mild steel, heat resistant steel, high carbon high chromium steel and cast iron. To understand the influence of wear deformation hardness test was conducted for all the target materials. Brinell hardness numbers for all target materials are tabulated in the Table1.

**Table 1: Brinell Hardness Number Of The Target Specimens**

| | Target specimens | Brinell hardness number |
|---|---|---|
| 1 | Mild steel | 130.9 |
| 2 | Heat resistant steel | 155.6 |
| 3 | High carbon high chromium steel | 158.2 |
| 4 | Cast iron | 159.3 |

## 3.2 Tribological Test

For understanding field conditions dry sand rubber abrader test was conducted. Two normal loads i.e., 53.2 N and 102.4 N were selected to conduct the test. Sand abrader was used available commercially in the nature. Weight loss of before the test and after the test was estimated by weighing the target specimens before and after the tests. Estimated volume loss was tabulated in the Table 2. Variability of volume loss versus hardness of all target materials was plotted and shown in the Figure 3.

Maximum weight loss of an amount of 0.8 was observed for a normal load of 102.4 N in mild steel. Minimum weight loss of an amount 0.6 was observed at a normal load of 102.4 N happened on cast iron. Weight loss of 0.4 is observed in the mild steel when the normal load changes from 102.4 N to 53.2 N. For a lower hardness the weight loss was found to be sensitive and this sensitiveness was gradually decreases when the hardness is goes on increasing with respect to the target materials. Finally, the weight loss was insensitive to the normal load when the hardness is at higher value within the experimental conditions.

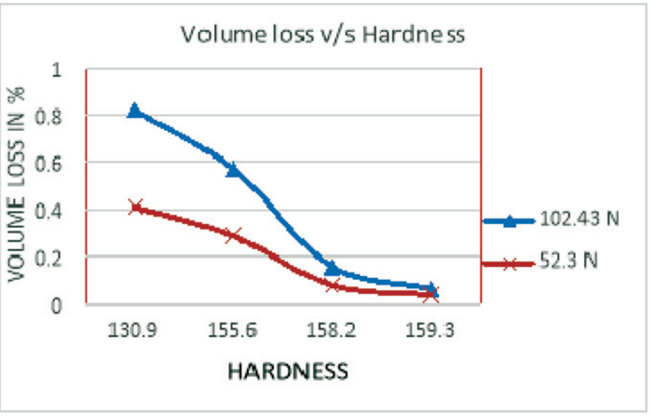


**Figure 3:** Dependency of volume loss on hardness with respect to two normal loads

**Table 2: Volume loss of target materials**

| | Target specimens | Percentage of weight loss for a load 53.2 N | Percentage of weight loss for a load 102.4 N |
|---|---|---|---|
| 01 | Mild steel | 0.41 | 0.82 |
| 02 | Heat resistant steel | 0.29 | 0.57 |
| 03 | High carbon high chromium steel | 0.08 | 0.16 |
| 04 | Cast iron | 0.04 | 0 .06 |

## 3.3 Scanning Electron Microscopy

Morphological analysis was done to identify the mode of wear Figure 6 shows wear scar of the target material mild steel when. There are two major observable grooves was found at the micrograph shown in Figure 4(a) at the normal load of 102.4 N, when viewed in the magnification of 2500x. It is also found that small scratches at the mid of the micrograph. Figure 4(b) shows the wear scar of mild steel at the normal load of 53.2N. Two grooves adjacent to each other was found at mid and edge of micrograph. At first groove knife edged ridge was found and smoother ridge was found at second groove. These features were found at the magnification of 3000x. Ridge found at second groove is not raised to that much but torn out at many places.

Sub-surface studies of target materials in scanning electron microscope were carried out for further understanding on inelastic deformations.

Micrographs shown in Figure 5(a) is the subsurface of mild steel target which was abraded with a normal load i.e.,

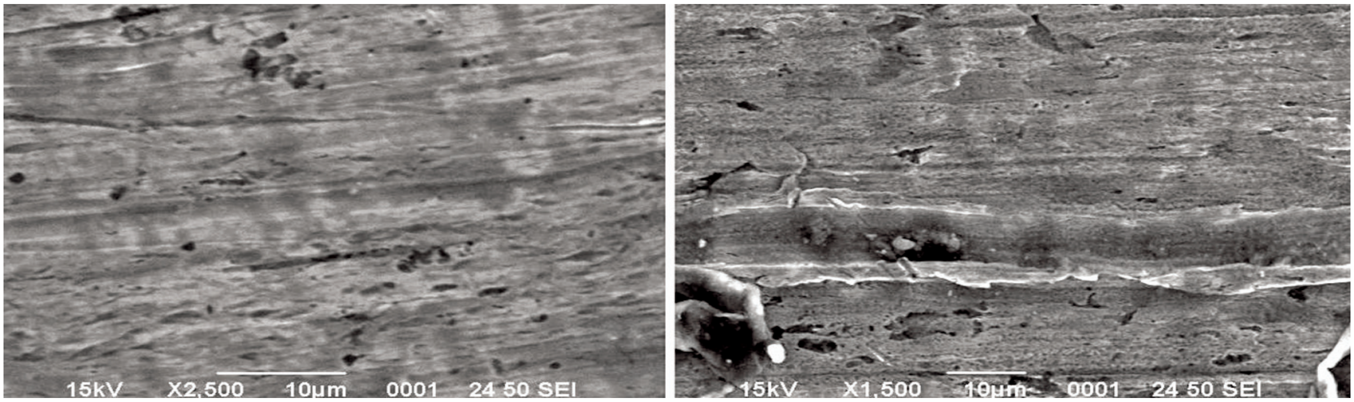


(a) (b)

**Figure 4:** Micrographs (SEM Images) of mild steel subjected to normal load of (a) 102.4N and (b) 53.2N in the magnification of 2500x and 3000x.

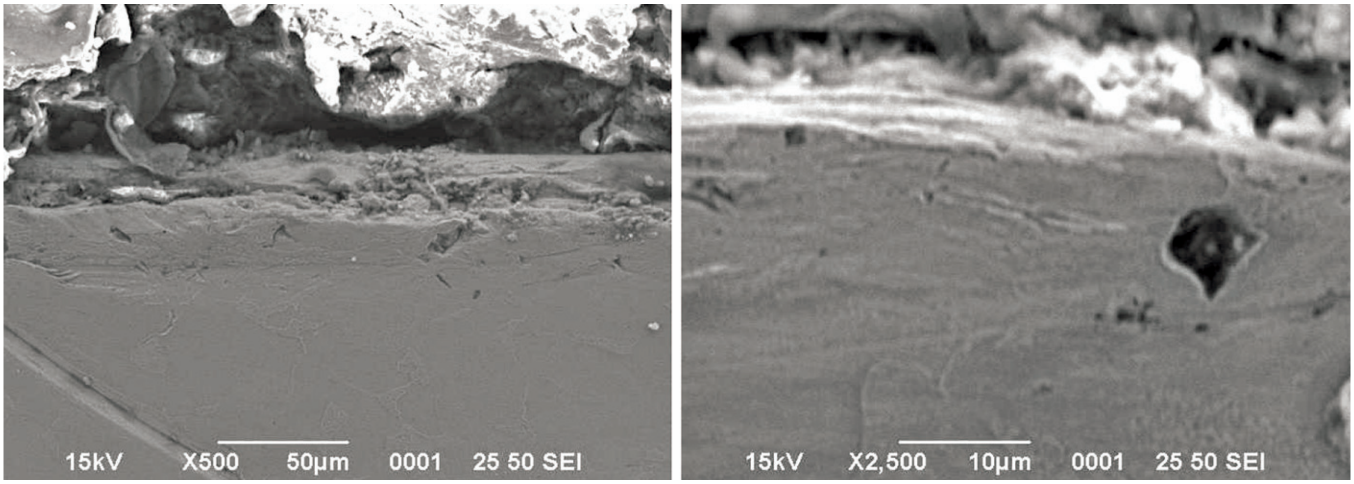


(a) (b)

**Figure 5:** Subsurface micrographs (SEM Images) of mild steel subjected to normal load of 53.2N (a) and 102.4N (b) in the magnification of 500x and 3000x

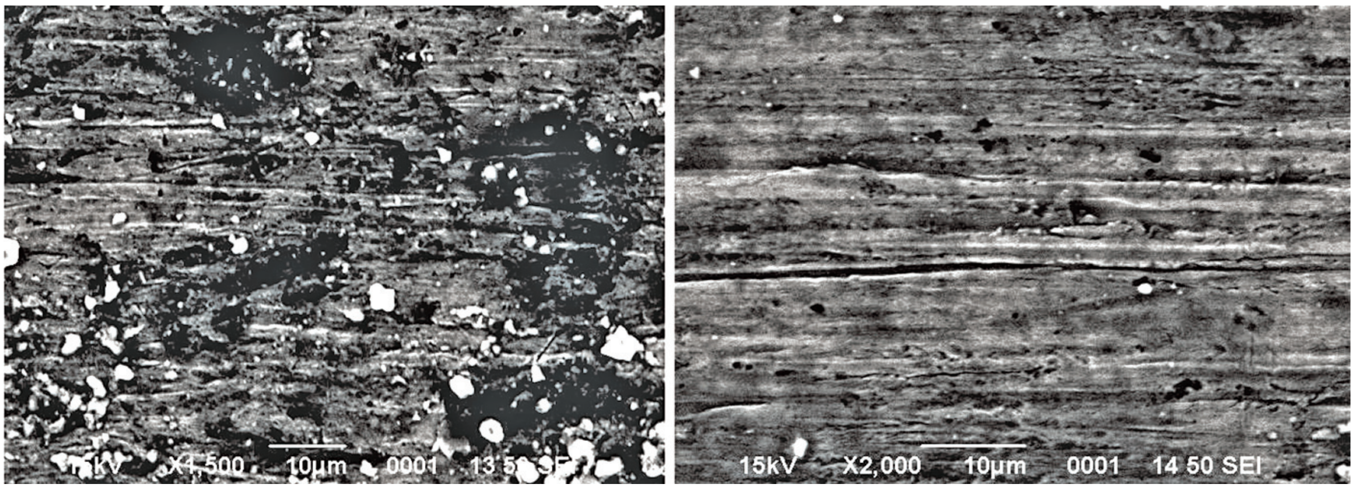


(a) (b)

**Figure 6:** Micrographs (SEM Images) of Heat Resistant steel subjected to normal load of 53.2N (a) and 102.4 N (b) in the magnification of 1500x and 2000x

52.3N. The feature in the micrograph does not show any subsurface inelastic deformation. Micrograph shown in Figure 5(b) of figure is the subsurface of mild steel target which was subject of normal load 102.4N. The feature in the image shows an extent of small magnitude of inelastic deformation.

Micrographs of wear scar of heat resistant steel are shown in micrograph of Figure 8. Many small grooves were found in the micrograph shown in Figure 6(a) at a normal load of 53.2N when viewed in the magnification of 1500 x. These grooves are distributed in the entire micrograph but not clearly defined. Micrograph shown in the Figure 6(b) is viewed in the magnification of 2000x at the normal load of 102.4N. Small amount of clearly defined grooves were observed at the mid of the micrograph. Little number of not cleared grooves are found at the other areas of the micrograph. Features of cutting mode of abrasive wear were slightly identified in the micrographs shown in Figure 6.

Micrograph shown in Figure 7(a) is the subsurface of heat resistant steel target which was abraded with a normal load i.e., 52.3N. The feature in the micrograph does not show any subsurface inelastic deformation. Micrograph shown in Figure 7(b) is the subsurface of heat resistant steel target which was abraded with a normal load of 102.4N. The feature in the micrograph reveals an extent of small magnitude of inelastic deformation. Cutting mode of abrasive wear mode was found.

Worn images of high carbon high chromium steel (HCHC)

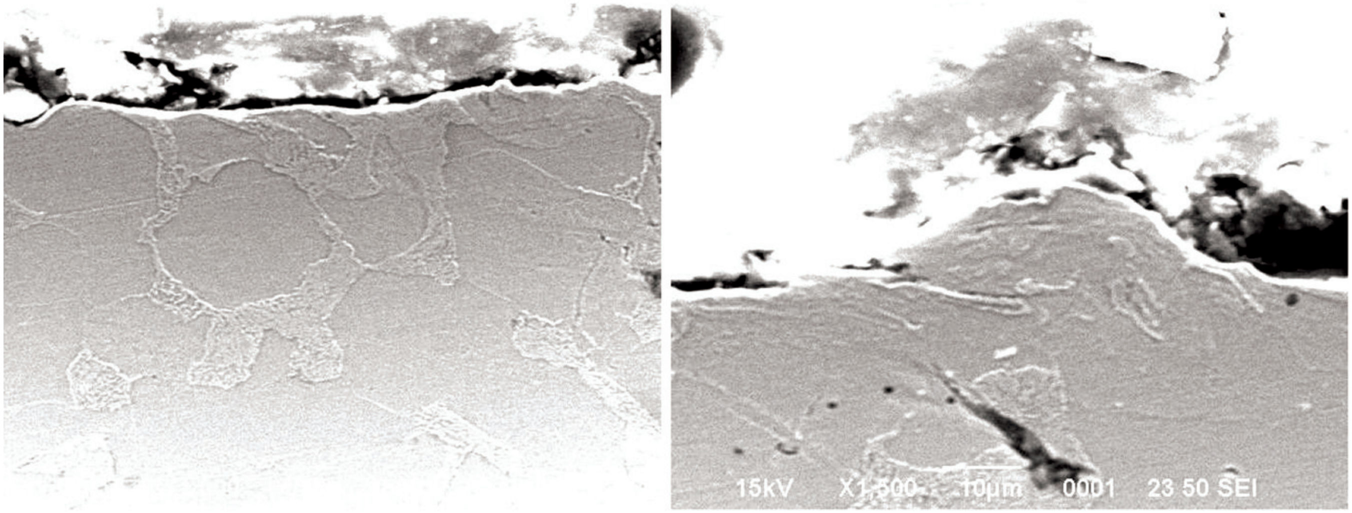


(a) (b)

**Figure 7:** Subsurface micrographs (SEM Images) of Heat Resistant steel subjected to normal load of 53.2N(a) and 102.4 N(b) in the magnification of 1500x and 2000x

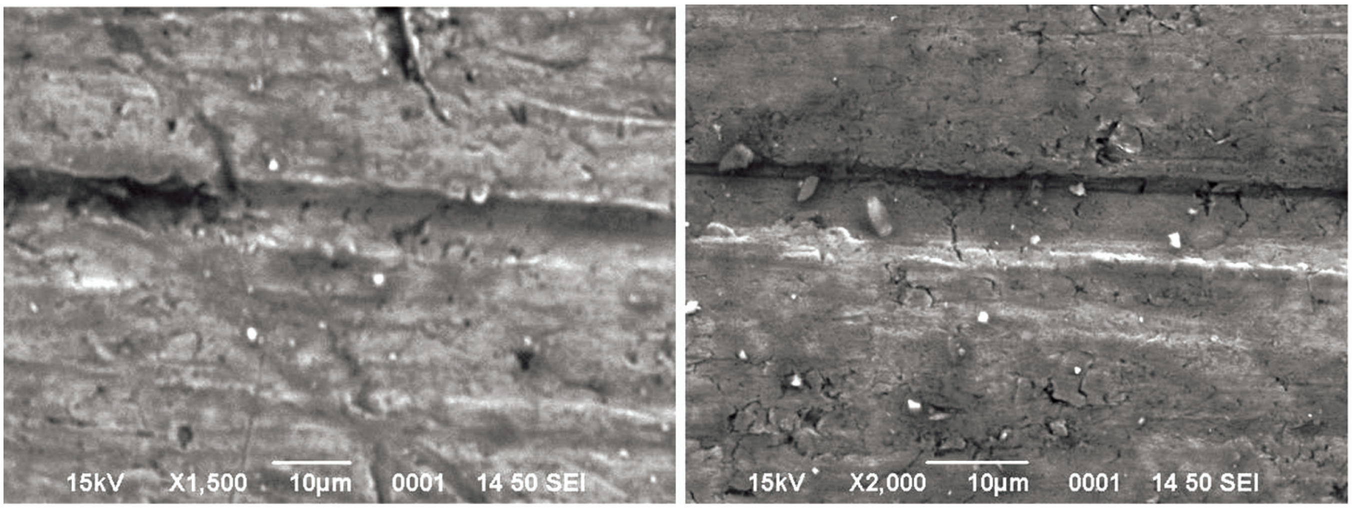


(a) (b)

**Figure 8:** Micrographs (SEM Images) of high carbon high chromium steel (HCHC) subjected to normal load of (a) 102.4N and (b) 53.2N in the magnification of 1500x and 2000x

is shown in micrograph of Figure 8. A big groove without any ridge in the smooth surface area was identified in the micrograph of Figure 8(a) in the magnification view 1500x. Counted number of small grooves are also found. Micrograph shown in the Figure 8(b) is viewed in the magnification of 2000x at the normal load of 102.4 N. Small amount of clearly defined grooves were observed at the mid of the micrograph. One well cleared groove without ridge was found at the middle of micrograph. Small numbers of cracks are also observed in the remaining area of the micrograph. Wedge mode of abrasive wear was found.

Micrograph shown in Figure 9(a) is the subsurface of high-carbon high-chromium steel target which was abraded with a load 52.3 N. The feature in the micrograph does not show any subsurface inelastic deformation. Micrograph shown in Figure 9(b) is the subsurface of high-carbon high-chromium steel target which was abraded with a normal load i.e., 102.4N. The feature in the image does not show any subsurface inelastic deformation.

Micrographs of wear scar of cast iron are shown in micrograph of Figure 10, Many shallow or narrow grooves were found in center and right-side of the micrograph shown

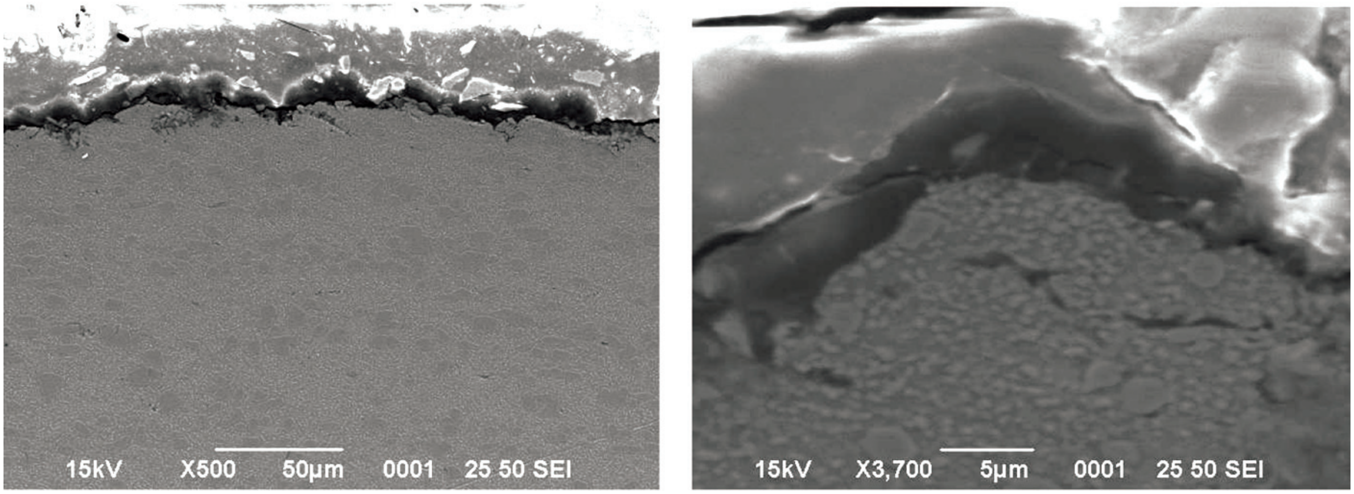


(a) (b)

**Figure 9:** Subsurface micrographs (SEM Images) of high carbon high chromium steel (HCHC) subjected to normal load of (a) 102.4N and (b) 53.2N

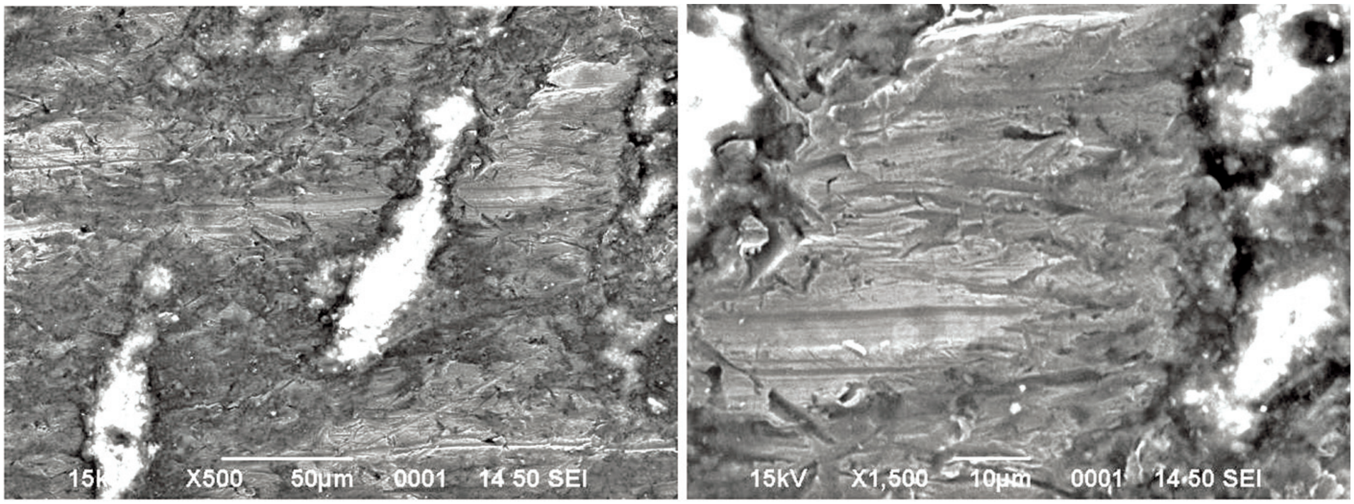


(a) (b)

**Figure 10:** Micrographs (SEM Images) of cast iron subjected to normal load of (a) 102.4N and (b) 53.2N

in Figure 10(a) at a normal load of 53.2N when viewed in the of 500x magnification. All these grooves are formed without any ridges. Micrograph shown in the Figure 10(b) is viewed in the magnification of 1500x at the normal load of 102.4N. Not through run-out grooves were found one behind with another. All these grooves are found without any ridges. Slight features of wedge mode abrasive wear were found.

Micrograph shown in Figure 11(a) is the subsurface of cast iron target which was abraded with a normal load i.e., 52.3N. The feature in the micrograph does not show any subsurface inelastic deformation. Micrograph shown in Figure 11(b) is the subsurface of cast iron target which was abraded with a normal load i.e., 102.4N. The feature in the micrograph does not show any subsurface inelastic deformation.

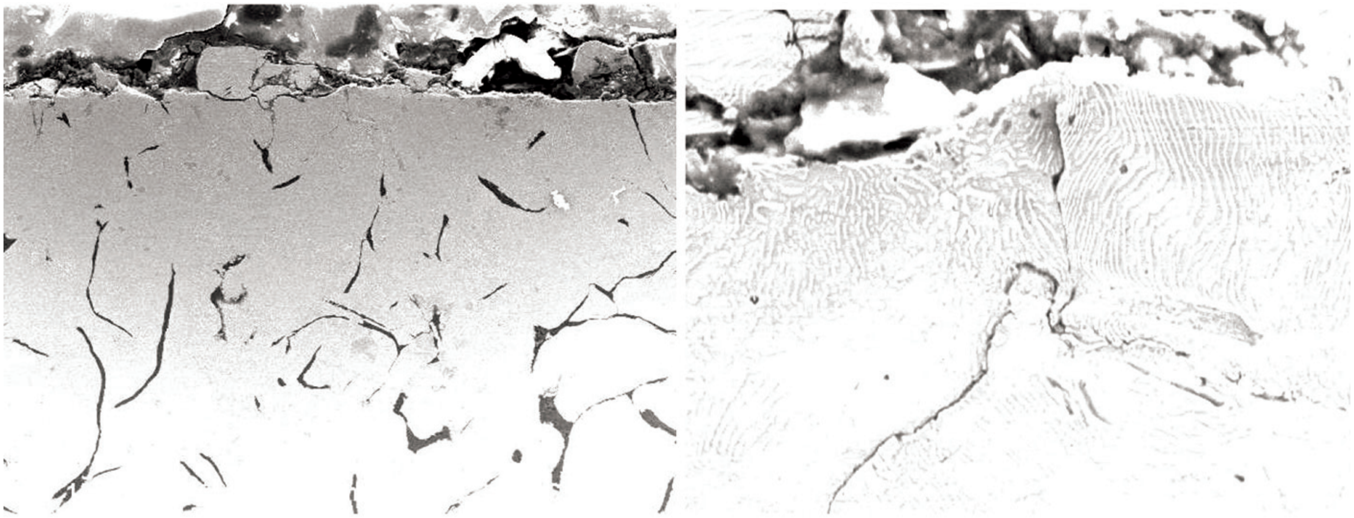

(a) (b)

**Figure 11:** Subsurface micrographs (SEM Images) of cast iron subjected to normal load of (a) 102.4N and (b) 53.2N

## 4.0 Conclusions

1. Identified wear was in the sequence of deformation happened with different modes of abrasive wear.
2. Cutting mode of abrasive wear was observed in mild steel and heat resistant steel
3. Wedge mode of abrasive wear was observed in high carbon high chromium steel and cast iron.
4. Maximum weight loss was found in mild steel and minimum weight loss was found in cast iron.
5. Comparable weight loss was observed in mild steel as well as in heat resistant steel. Comparable weight loss was found both in high carbon high chromium steel and cast iron.
6. Observable plastic deformation was found in mild steel and light amount of plastic deformation in heat resistant steel, high carbon and high chromium steel and cast iron.

## References


1. Archard, J.F, J. Appl. Phys.,1953, 24, 981-988.
2. Bhansali, K. J, wear control hand book, Peterson M.B and Winer, W.O (Eds), 1980, ASME, 373-383.
3. Johnson, K. L., Wear, 1994, 190, 162-170.
4. Hokkarigawa, K., *Bulletin of the ceramic society of Japan*, 1997, 19-24.
5. Holm, R., Electric contact, Almquist and Wiksells, Stockhelm, 1946, section 40.
6. Lancaster, J.K., *Trans. Inst. Metal Finish,* 1978, 56, 4, 145.
7. Rabincowicz, E., Wear control hand book, Peterson M.B and Winer, W.O, (Eds), ASME, 1980, 475.
8. Lim, S.C. and Ashby, M.F., *Acta Metallurgica*, 1987, 35, 1, 1-24.
9. Hokkarigawa, K and Kato, K., *Tribology Int.*, 1988, 21, 1, 51-57.
10. M.S Bingley, S. Schnee, *Wear*, 2005, 258, 50-61.
11. Yefei Li, Yimin Gao, *Wear* 268 (2010), 511-518.
12. Cho, S. J., Hockey, B. J., and Lawn, B.R. (), *J. Am. Ceram, Soc.*, 1989, 72, 7, 1949-1952.